BIOCHEMISTRY
including biophysical chemistry & molecular biology

Article

pubs.acs.org/biochemistry

Redox and Metal Ion Binding Properties of Human Insulin-like Growth Factor 1 Determined by Electrospray Ionization Mass Spectrometry

Julia Smirnova, Jekaterina Muhhina, Vello Tõugu, and Peep Palumaa*

Department of Gene Technology, Tallinn University of Technology, Akadeemia tee 15, 12618 Tallinn, Estonia

ABSTRACT: Insulin-like growth factor 1 (IGF-1) is a 70-residue hormone containing three intramolecular disulfide bridges. IGF-1 and other growth factors are oxidatively folded in the endoplasmic reticulum and act primarily in the blood, under relatively oxidative conditions. It is known that IGF-1 exists in various intracellular and extracellular compartments in the oxidized form; however, the reduction potential of IGF-1 and the ability of fully reduced IGF-1, which contains six cysteine residues, to bind transition metal ions are not known. In this work, we determine that the redox potential of human IGF-1 is equal to −332 mV and the reduced form of hIGF-1 can bind cooperatively four Cu^+ ions, most probably into a tetracopper−hexathiolate cluster. The Cu^+ binding affinity of hIGF-1 is, however, approximately 3 times lower than that for the copper chaperones; thus, we can conclude that fully reduced hIGF-1 cannot compete with known Cu^+-binding proteins.

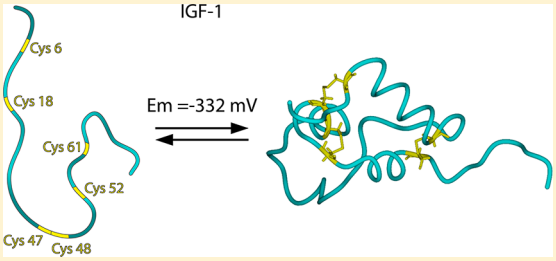

Insulin-like growth factor 1 (IGF-1), a 70-residue hormone (7649 Da) displaying a high degree of homology to insulin, consists of three intramolecular disulfide bridges.[1] Although small amounts of IGF-1 are synthesized in most peripheral tissues, it is mainly secreted by the liver. The secretion of IGF-1 is regulated by growth hormone (GH).[2] The major part of IGF-1 circulating in the bloodstream is in the complex with one of six IGF-binding proteins (insulin-like growth factor binding proteins 1−6 or IGFBP1−6),[3,4] and only a small amount of IGF-1, <1%, circulates in the free biologically active form that can bind to the IGF receptor.[5] All three native disulfide bridges in the IGF-1 molecule are crucial for this binding.[6]

Before it is released into the blood, IGF-1 is oxidatively folded in the endoplasmic reticulum (ER). Both these environments, blood and ER, are characterized by oxidative redox potentials. On the basis of the experimental determination of the GSH/GSSG ratio, the average redox potential in the ER is estimated to be equal to −189 mV.[7] The oxidative conditions in the ER guarantee the formation of structural disulfide bridges in the membrane and extracellular proteins during protein folding.[8] The redox potential values in the extracellular environments are also determined by thiol−disulfide equilibria. The main redox couple in this environment, Cys/CySS, plays a major role in the redox communication between cells and tissues.[9−12] The Cys/CySS buffering system keeps the mean plasma redox potential value at approximately −80 mV, whereas the mean plasma redox potential value, which is determined by the GSH/GSSG ratio, is approximately −140 mV.[13,14] Both values are substantially higher (more oxidizing) than the cytoplasmic redox potential values. The redox potential value of plasma becomes more oxidative during several diseases and aging, and these changes have been shown to affect the function of cell surface receptors, ion channels, and structural proteins.[13,15] It should be noted that the plasma Cys/CySS redox potential is not in equilibrium with the plasma GSH/GSSG pool.[16]

The disulfide bonds in the proteins can be classified as stable structural disulfide bridges with midpoint redox potentials reaching −470 mV[17] and as the more labile redox-active disulfides with corresponding midpoint redox potentials ranging from −95 to −330 mV.[18−21] The disulfide bonds in IGF-1 most probably belong to the structural ones; however, their reduction in the cellular cytosol cannot be ruled out. The highly reducing cellular redox potential with values as low as −289 mV[22] is maintained mainly by the redox couple of GSH and GSSG, with a total cellular concentration of 2−10 mM.[23] The cellular redox potential value is different in various organelles and fluctuates depending on the cell cycle and apoptotic processes, the presence of ROS and RNS, and the state of disease or aging.[14] The redox potential of the cytoplasm has been reported to be in the range from −193 mV for the red blood cells[24] to −220 mV for nondividing cells and −260 mV for proliferating cells.[14] The state of cellular thiols depends primarily on the environmental redox potential and the presence of ROS or RNS.

If IGF-1 becomes reduced, it can bind metal ions and, in particular, Cu^+ ions. It has been demonstrated that Cu^+ ions can bind to proteins containing six Cys residues with high affinity, forming tetracopper−hexathiolate clusters.[25−27] Fully reduced IGF-1 is a good model for such proteins, and the Cu^+

Received: April 17, 2012
Revised: June 29, 2012
Published: July 2, 2012

dx.doi.org/10.1021/bi300494s | *Biochemistry* 2012, 51, 5851−5859

binding affinity of reduced IGF-1 allows the estimation of whether such proteins can compete with cellular Cu^+ proteins.

In this work, we applied a recently developed ESI-MS method[28] to IGF-1 and demonstrated that the disulfide bonds in this molecule are formed in a cooperative manner with a midpoint redox potential value equal to −332 mV. This value is sufficiently low in comparison with the redox potentials of the secretory pathway and extracellular environment for stabilizing hIGF-1 in its fully oxidized native fold that is required for IGFR binding. Fully reduced hIGF-1 binds four Cu^+ ions with very high cooperativity, suggesting the formation of a tetracopper−hexathiolate cluster. In principle, the interaction with metal ions can stabilize the reduced form of the peptide; however, the Cu^+ binding affinity of hIGF-1 is 3-fold weaker than that of the copper chaperone Cox17,[25] which has the lowest affinity for copper among the proteins forming the cellular copper proteome.[29] Thus, formation of the Cu^+−IGF-1 complex in the cellular environment is improbable.

MATERIALS AND METHODS

Chemicals. Human insulin-like growth factor 1 (hIGF-1) (ProSpec), DTT (Fluka), BME (Sigma), oxidized BME (Aldrich), Cu(II) acetate (Sigma), and ammonium acetate (Scharlau) were acquired. Oxidized DTT was synthesized from reduced DTT according to the protocol described in ref 30. Milli-Q quality water was used for the preparation of solutions.

Reduction of hIGF-1 with DTT. Fully oxidized human IGF-1_{3S-S} (2 μM) was incubated in argon-saturated 20 mM ammonium acetate (pH 7.5), containing 0.5, 1, and 5 mM DTT as a reducing agent. Separate reaction mixtures were incubated at 25 and 40 °C. For the measurement of kinetics of IGF-1_{3S-S} reduction, 50 μL aliquots from the reaction mixture were taken at various time points (1−120 min) and injected directly by a syringe pump at a rate of 10 μL/min into a QSTAR Elite ESI-Q-TOF mass spectrometer (Applied Biosystems, Foster City, CA). Mass spectra were recorded in the positive mode over 2−3 min in the region from 500 to 2000 Da. The following instrument parameters were used: ion spray voltage, 5500 V; source gas, 30 L/min; curtain gas, 20 L/min; declustering potential, 60 V; focusing potential, 320 V; ion release delay, 6; ion release width, 5; detector voltage, 2300 V. The obtained spectra were deconvoluted and analyzed using Bioanalyst version 2.0 from Applied Biosystems.

The rate constant (k) for hIGF-1_{3S-S} reduction with 0.5, 1, and 5 mM DTT was calculated from kinetic data at different temperatures using the exponential equation

$$y = A_1 - A_2 e^{-kt} \quad (1)$$

where k is the rate constant, y is the average molecular mass of hIGF-1, t is the incubation time, and A_1 and A_2 are constants. Data were fit using an A_1 of 7648.5 (molecular mass of hIGF-1_{3S-S}) and an A_2 of 7654.5 (molecular mass of hIGF-1_{0S-S}) with Origin 6.1 (Originlab Corp., Northampton, MA).

The half-life of the reaction is equal to

$$t_{1/2} = \ln(2)/k \quad (2)$$

Reduction of hIGF-1 with BME. Fully oxidized human IGF-1_{3S-S} (2 μM) was incubated in argon-saturated 20 mM ammonium acetate (pH 7.5), containing 5, 10, and 25 mM BME as a reducing agent.

The reaction mixtures were incubated at 25 or 40 °C. At various time points (1−300 min), aliquots from the reaction mixture were analyzed by ESI-MS as described above.

Measuring the Redox Potential of hIGF-1 in DTT/DTT_{ox} and BME/BME_{ox} Redox Buffers. For the measurement of the redox potential of hIGF-1, fully oxidized hIGF-1_{3S-S} (2 μM) was incubated in various DTT- and BME-based redox buffers to achieve the redox equilibrium between the protein forms. The equilibrium ratios of hIGF-1 redox forms were determined after incubation of hIGF-1_{3S-S} (2 μM) for 30 min at 40 °C in DTT/DTT_{ox} redox buffers ([DTT] + [DTT_{ox}] = 5 mM) or after incubation of hIGF-1_{3S-S} (2 μM) for 3 h at 40 °C in BME/BME_{ox} redox buffers ([BME] + 2[BME_{ox}] = 25 mM) by ESI-MS.

The fractional content of IGF-1_{0S-S} was determined by dividing the mass increment (average molecular mass of hIGF-1 minus molecular mass of IGF-1_{3S-S}) by 6 (maximal mass increment in the case of reduction of three S−S bonds).

The redox potential of redox buffers was adjusted by varying the ratio of reduced and oxidized forms of DTT and BME, and corresponding redox potentials were calculated from the following Nernst equations:

$$E' = E_0'(\mathrm{DTT}) - [(RT)/(nF)] \ln([\mathrm{DTT}]/[\mathrm{DTT_{ox}}]) \quad (3)$$

$$E' = E_0'(\mathrm{BME}) - [(RT)/(nF)] \ln([\mathrm{BME}^2]/[\mathrm{BME_{ox}}]) \quad (4)$$

where E_0'(DTT) = −0.323 V (pH 7.0 and 25 °C),[31] E_0'(BME) = −0.231 V (pH 7.0 and 25 °C),[32] R is the gas constant (8.315 J K^{-1} mol^{-1}), n is the number of electrons transferred in the reaction, and F is the Faraday constant (9.6485×10^{-4} C mol^{-1}). The E_0'(DTT) and E_0'(BME) values have been recalculated for 40 °C using eqs 3 and 4 and for pH 7.5 using the following equation:

$$E_{pH} = E_0' + (\mathrm{pH} - \mathrm{pH_0})(\Delta E/\Delta \mathrm{pH}) \quad (5)$$

where $\Delta E/\Delta$pH is the change in E if the pH is increased by 1 unit and is equal to 60.1 mV.[33]

The midpoint redox potential of the hIGF-1_{3S-S} → hIGF-1_{0S-S} reaction was determined by fitting the fractional content of hIGF-1_{0S-S} to the equation

$$y = (A_1 - A_2)/[1 + e^{(x-x_0)/dx}] + A_2 \quad (6)$$

where y is the fractional content of hIGF-1_{0S-S}, x is the environmental redox potential (E_h), A_1 and A_2 are constants, and x_0 is the midpoint redox potential (E_m). Data were fit using an A_1 of 0 (initial fractional content of hIGF-1_{0s-s}) and an A_2 of 1 (final fractional content of IGF-1_{0s-s}) with Origin 6.1 (Originlab Corp.).

Copper Binding Properties of hIGF-1 Reduced with DTT and BME and Stability of Cu^+−Protein Metalloforms in the Presence of Increasing Concentrations of DTT. Human IGF-1 was reduced using one of the following schemes. hIGF-1 (2 μM) was fully reduced at 40 °C with 0.5 mM DTT for 90 min, and 10 μM hIGF-1 was partially reduced with 10 mM BME at 40 °C for 220 min. Reduction was confirmed by ESI-MS. Metal binding experiments were performed with partly reduced and fully reduced hIGF-1 forms. Reconstitution of various IGF-1 forms with copper was performed as follows. First, Cu(II) acetate was dissolved at a concentration of 100 μM in argon-saturated 20 mM ammonium acetate (pH 7.5), and Cu^{2+} was reduced to Cu^+ by the addition of 0.5 mM DTT or 1 mM BME. A freshly prepared metal salt

dx.doi.org/10.1021/bi300494s | Biochemistry 2012, 51, 5851−5859

solution (1−8 equiv) was added to apoIGF-1, and the mixture was incubated for 1 min at 25 °C. Samples were then diluted with 20 mM ammonium acetate (pH 7.5) to a final protein concentration of 1 μM (final concentration of reducing agent in the final sample for MS of 0.5 mM for DTT and 1 mM for BME) and infused with a syringe pump into a QSTAR Elite ESI-Q-TOF mass spectrometer at a rate of 10 μL/min.

The influence of DTT on copper binding by hIGF-1 was studied by adding of 0.5−7.5 mM reduced DTT to 1 μM Cu_nIGF-1. Cu_nIGF-1 was prepared by addition of 8 equiv of the Cu^+DTT complex to hIGF-1. The Cu^+DTT complex was prepared by addition of DTT to copper acetate at a concentration of 16 μM in argon-saturated 20 mM ammonium acetate (pH 7.5). Final mixtures contained 0.25−4 mM DTT and 1 μM Cu_nIGF-1. The obtained mixtures were injected into the QSTAR Elite ESI-Q-TOF instrument.

Characterization of hIGF-1 via High-Performance Liquid Chromatography (HPLC). hIGF-1 (25 μL of 30 μM hIGF-1) was applied to a reversed-phase HPLC column (Agilent Eclipse XDB-C18, 4.6 mm × 150 mm, 5 μm) and analyzed according to the method described by Miller and colleagues[34] with small modifications. The gradient used for all HPLC experiments was as follows: (i) equilibration of the column with 80% A [0.1% (v/v) aqueous trifluoroacetic acid] and 20% B [88% acetonitrile, 2% 2-propanol, 9.9% water, and 0.1% trifluoroacetic acid (all v/v)], (ii) a linear gradient to 30% B in 1 column volume (CV), (iii) a linear gradient to 38% B in 8.4 CV, and (iv) a linear gradient to 80% B in 6.2 CV. After each run, the column was washed with 100% B and re-equilibrated.

Disulfide rearrangement was performed according to the method described in ref 34 with small modifications. hIGF-1 (30 μM) was incubated with BME at a BME/IGF-1 ratio of 13/1 in 20 mM ammonium acetate (pH 7.5) at 25 °C for 23 h and subjected to HPLC.

For redox experiments, hIGF-1 was incubated in different DTT/DTT_{ox} redox buffers as described in the ESI-MS section and chromatographed after incubation for 1 h. E_h values of the samples were established via calculation of the DTT/DTT_{ox} ratios of the corresponding DTT and DTT_{ox} peaks, which had been resolved in each HPLC chromatogram. In the incubation mixtures, the concentration of DTT and DTT_{ox} was 75 mM, and the concentration of IGF-1 was 30 μM.

All peaks present in HPLC chromatograms were collected and identified using ESI-MS.

RESULTS

Reduction of hIGF-1 with DTT. The mass spectrum of isolated hIGF-1 showed three major peaks with charges of +5, +6, and +7 with different distributions in samples containing oxidized and reduced forms of the protein. The average molecular mass of hIGF-1 was calculated using all peaks corresponding to different ionization states in the particular sample. High-resolution ESI-MS spectra of hIGF-1 (Figure 1) show a small increase in the protein molecular mass in the presence of DTT.

The deconvolution of the spectrum in the absence of DTT gave a molecular mass of 7648.66 Da that agrees well with the theoretical molecular mass of oxidized hIGF-1 containing three disulfide bridges (7648.70 Da). Incubation of fully oxidized hIGF-1 with 0.5 mM DTT at 25 and 40 °C for 120 min resulted in gradual reduction of the protein reflected in progressive increase in its molecular mass. The increase in the average molecular mass of hIGF-1 was 6 Da (Figure 2), which

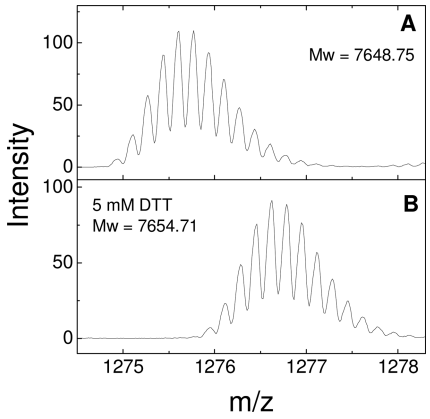

Figure 1. High-resolution ESI-MS spectra of hIGF-1 in the absence and presence of DTT. Conditions: 2 μM hIGF-1, 20 mM ammonium acetate, pH 7.5. (A) hIGF-1 or (B) hIGF-1 incubated with 5 mM DTT at 40 °C for 45 min. The +6 charge states are presented, and average molecular masses were calculated using Bioanalyst.

corresponds to the reduction of all three disulfide bonds. The incubation of hIGF-1_{3S-S} at higher concentrations of DTT at 25 and 40 °C led to the fast reduction of the protein (approximately 15 min for 5 mM DTT and 45 min for 1 mM DTT for the full reduction of the protein). Fully reduced hIGF-1 exposes four ion species (charges from +5 to +8) in the mass spectrum. Figure 2 shows that all three disulfide bonds are reduced simultaneously because the kinetic curve of the increase of the protein molecular mass can be fit to a single exponent. The half-life ($t_{1/2}$) of the reaction varied between 1.9 and 27.1 min depending on the incubation temperature and concentration of DTT.

Reduction of hIGF-1 with BME. The acquired ESI mass spectra of hIGF-1 displayed three main peaks with charges of +5, +6, and +7. In the presence of BME, an additional minor peak corresponding to the hIGF-1_{1S-S}−BME adduct was also detected. Incubation of hIGF-1_{3S-S} with 25 mM BME resulted in an increase in the average molecular mass of hIGF-1 of ∼5 Da (Figure 3), which corresponds to the reduction of two or three disulfide bonds.

Reduction of hIGF-1_{3S-S} with 5 mM BME occurs with a half-life of 22 min at 40 °C and 37 min at 25 °C, whereas increasing the BME concentration to 10 and 25 mM at 40 °C shortened the half-lives to 8 and 2.4 min, respectively.

The reduction of hIGF-1 by BME is considerably slower than its reduction by DTT under similar conditions; however, at a high (25 mM) concentration of BME and an elevated temperature (40 °C), the reaction occurs much faster (half-life of ∼2 min) and all disulfide bonds are reduced (Figure 3). Reduction occurs at a slightly lower rate comparable to that with DTT; however, disulfide bonds were reduced simultaneously, as in the case of DTT.

Determination of Midpoint Redox Potentials of hIGF-1 in DTT/DTT_{ox} and BME/BME_{ox} Redox Buffers. Figure 4A shows the dependence of the average mass of hIGF-1 on the redox potential in 5 mM DTT/DTT_{ox} redox buffers determined after incubation at 40 °C for 30 min. The average mass of hIGF-1_{3S-S} increased by 6 Da at environmental redox potential values of less than −300 mV, which reflects the equilibrium position between hIGF-1_{3S-S} and hIGF-1_{0S-S} forms. The midpoint redox potential value for the hIGF-1_{0S-S}−hIGF-1_{3S-S} transition was calculated from the dependence of the fractional

dx.doi.org/10.1021/bi300494s | Biochemistry 2012, 51, 5851−5859

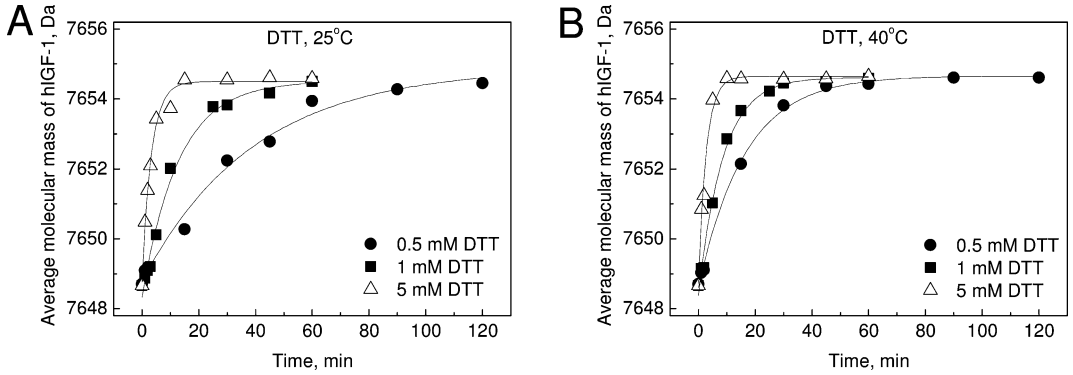

Figure 2. Kinetics of hIGF-1_{3S-S} reduction with DTT monitored by the increase in the average molecular mass of hIGF-1. Conditions: 2 μM hIGF-1_{3S-S}, 20 mM ammonium acetate, pH 7.5. (A) T = 25 °C, with 0.5, 1, and 5 mM DTT. (B) T = 40 °C, with 0.5, 1, and 5 mM DTT. Average molecular masses were calculated using Bioanalyst. Solid lines are fitted curves.

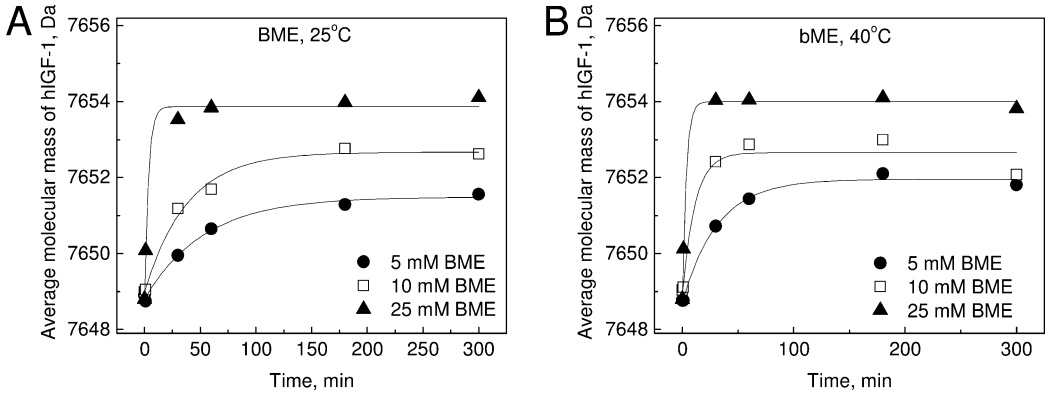

Figure 3. Kinetics of reduction of hIGF-1_{3S-S} by BME monitored by the increase in the average molecular mass of hIGF-1. Conditions: 2 μM hIGF-1_{3S-S}, 20 mM ammonium acetate, pH 7.5. (A) T = 25 °C, with 5, 10, and 25 mM BME. (B) T = 40 °C, with 5, 10, and 25 mM BME. Average molecular masses were calculated using Bioanalyst. Solid lines are fitted curves.

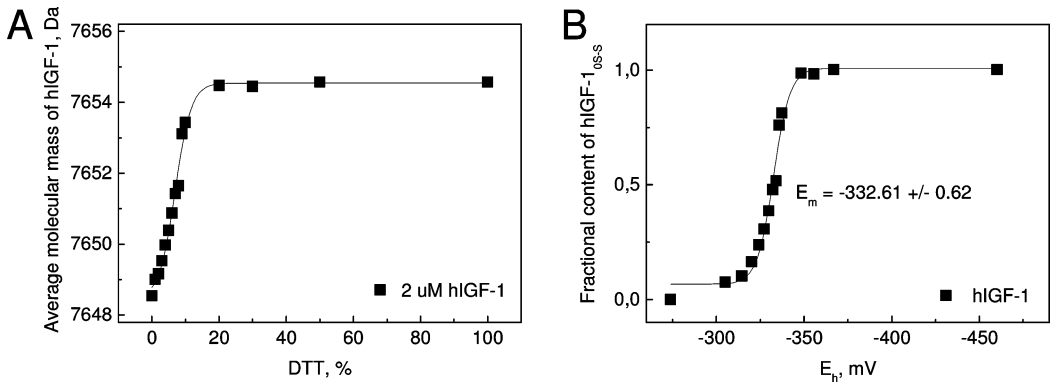

Figure 4. Determination of the redox midpoint potential of hIGF-1 in DTT/DTT_{ox} redox buffers. (A) Average molecular mass of hIGF-1 plotted vs increasing DTT concentrations in 5 mM DTT/DTT_{ox} redox buffers. (B) Fractional content of hIGF-1_{0S-S} at different E_h values generated by the DTT/DTT_{ox} couple.

content of hIGF-1_{0S-S} and E_h, presented in Figure 4B. The fitting of data to eq 6 yielded a midpoint redox potential equal to −332.61 ± 0.62 mV (pH 7.5 and 40 °C).

The average masses of hIGF-1 in 25 mM BME/BME_{ox} redox buffers determined after incubation at 40 °C for 3 h are presented in Figure 5A. At environmental redox potential values of less than −300 mV, the average mass of hIGF-1_{3S-S} increases 5−6 Da. The midpoint redox potential value for the hIGF-1_{0S-S}/hIGF-1_{3S-S} couple was calculated from the dependence of the fractional content of hIGF-1_{0S-S} from E_h, presented in Figure 5B. The fitting of the data to eq 6 yielded an E_m of −328.07 ± 1.01 mV (pH 7.5 and 40 °C), which is in agreement with the value observed in DTT/DTT_{ox} redox buffer because their confidence intervals overlap.

Copper Binding Properties of Reduced hIGF-1 and Stability of Cu^+−Protein Metalloforms in the Presence of Increasing Concentrations of DTT. Figure 6 shows the mass spectra of fully reduced IGF-1 at different concentrations of Cu^+ ions in the presence of 0.5 mM DTT. The addition of 1−2 equiv of Cu^+ ions to apoIGF-1 generated small amounts of two metalloforms of hIGF corresponding to Cu_4IGF-1 and Cu_4IGF-1-DTT (Figure 6A,B). After the addition of 4 and 6

dx.doi.org/10.1021/bi300494s | Biochemistry 2012, 51, 5851−5859

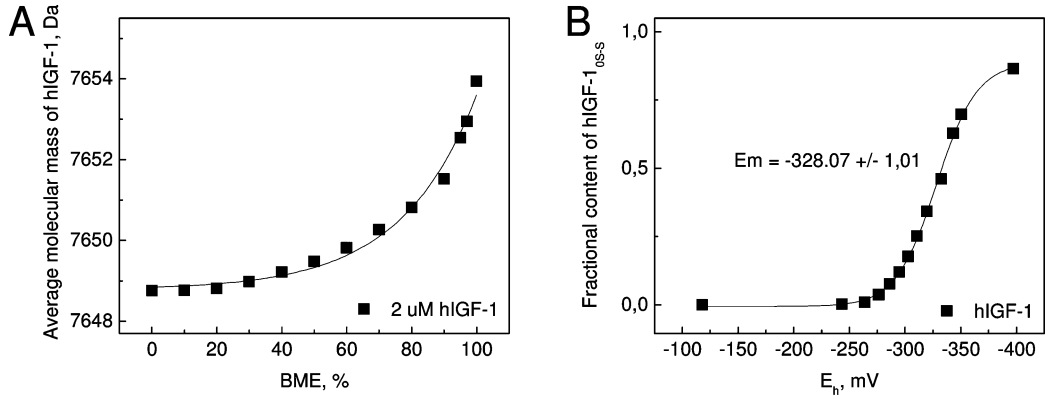

Figure 5. Determination of redox midpoint potentials of hIGF-1 in BME/BME_{ox} redox buffers. (A) Average molecular mass of hIGF-1 plotted vs increasing BME concentrations in 25 mM BME/BME_{ox} redox buffers. (B) Fractional content of hIGF-1_{0S-S} at different E_h values generated by the BME/BME_{ox} couple.

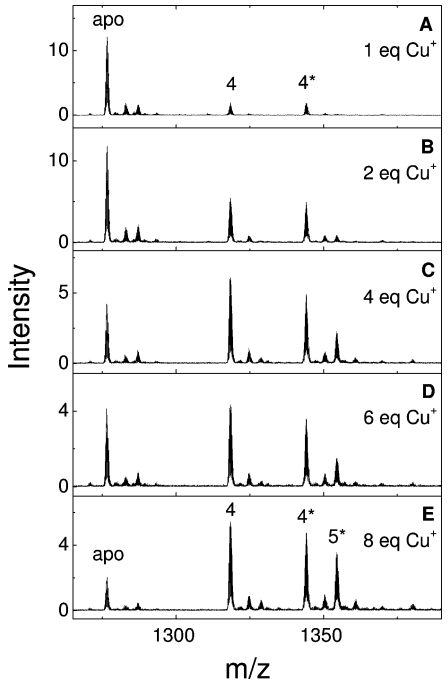

Figure 6. Binding of Cu^+ ions to hIGF-1 in the presence of DTT. Mass spectra of hIGF-1 (1 μM) reconstituted with 1−8 equiv of Cu^+ ions in the presence of 20 mM ammonium acetate (pH 7.5) and 0.5 mM DTT at 25 °C. Charge state +6 ions are presented, and numbers on the peaks denote the metal stoichiometry of the complex; asterisks denote DTT adducts.

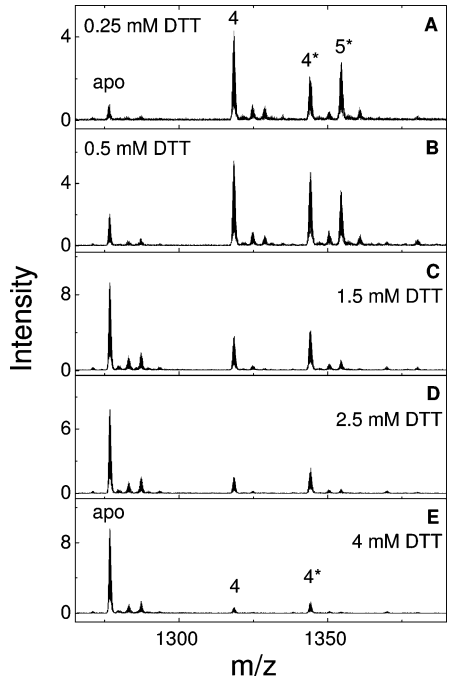

Figure 7. Release of Cu^+ ions in the presence of increasing concentrations of DTT. Mass spectra of hIGF-1 (1 μM) reconstituted with 8 equiv of Cu^+ ions in 20 mM ammonium acetate (pH 7.5) in the presence of DTT at various concentrations: (A) 0.25, (B) 0.5, (C) 1.5, (D) 2.5, and (E) 4 mM. Charge state +6 ions are presented, and numbers on the peaks denote the metal stoichiometry of the complex; asterisks denote DTT adducts.

equiv of Cu^+ ions, the MS spectrum exposes one dominant peak corresponding to Cu_4IGF-1 together with minor apoIGF-1, Cu_4IGF-1-DTT, and Cu_5IGF-1-DTT forms (Figure 6C,D). Addition of 8 equiv of Cu^+ ions leads to the relative increase in the magnitude of the Cu_5IGF-1-DTT peak and the decrease in the magnitude of the apoIGF-1 peak (Figure 6E). The experimentally determined molecular mass of Cu_4IGF-1 (7904.54 Da) indicates that the molecular mass of hIGF-1 in this complex is 7654.84 Da, which is very close to the theoretical value for the fully reduced hIGF-1 protein (7654.7 Da), demonstrating the absence of disulfide bridges in Cu_4IGF-1.

Figure 7 shows the mass spectra of hIGF-1 incubated with 8 equiv of Cu^+ in the presence of increasing concentrations of DTT. At 0.5 mM DTT, the peak corresponding to apoIGF-1 starts to increase (Figure 7B) and becomes dominant at 2.5 mM DTT (Figure 7D,E). The results demonstrate that DTT extracts metals from hIGF-1 at supramillimolar concentrations.

Mass spectra of hIGF-1, reduced with BME and reconstituted at pH 7.5 with increasing concentrations of Cu^+ ions in the presence of 1 mM BME, are presented in Figure 8. The MS spectrum in the presence of 1 equiv of Cu^+ exposes one major peak of Cu_4IGF-1 together with minor apoIGF-1 and Cu_4IGF-1-BME forms (Figure 8A). The magnitude of the apoIGF-1 peak decreases with elevated copper concentrations, and the peak became a minor form after the addition of 6 equiv of Cu^+ ions, where the MS spectrum exposes Cu_4IGF-1 as a major peak together with minor apoIGF-1, Cu_4IGF-1-BME, and Cu_5IGF-1 forms (Figure 8D). Further addition of Cu^+ ions leads to a relative increase in the magnitude of the Cu_5IGF-1

dx.doi.org/10.1021/bi300494s | Biochemistry 2012, 51, 5851−5859

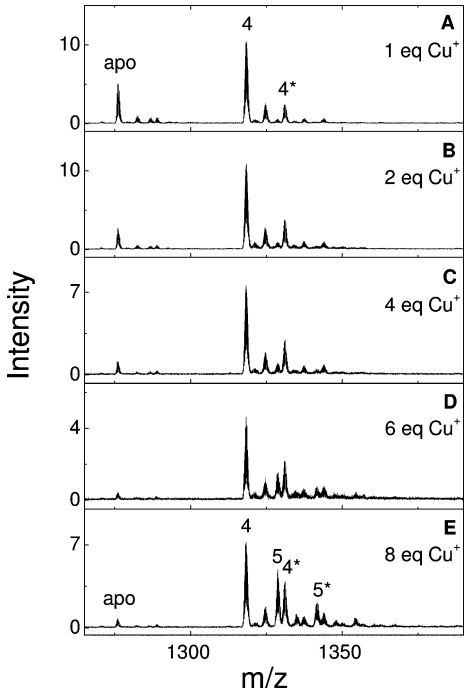

Figure 8. Binding of Cu^+ ions to hIGF-1 in the presence of BME. Mass spectra of hIGF-1 (1 μM) reconstituted with 1−8 equiv of Cu^+ ions in 20 mM ammonium acetate (pH 7.5) in the presence of 1 mM BME at 25 °C. Charge state +6 ions are presented, and numbers on the peaks denote the metal stoichiometry of the complex; asterisks denote BME adducts.

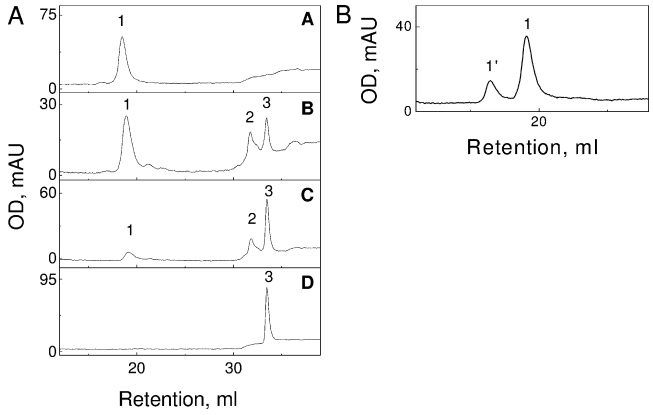

Figure 9. Disulfide rearrangement and redox properties of hIGF-1 monitored by HPLC. Conditions: 30 μM hIGF-1, 20 mM ammonium acetate, pH 7.5. (A) hIGF-1 (A), hIGF-1 incubated in DTT/DTT_{ox} redox buffer containing 2.6% DTT at 25 °C for 1 h (B), hIGF-1 incubated in DTT/DTT_{ox} redox buffers containing 5% DTT at 25 °C for 1 h (C), and hIGF-1 incubated with DTT at 25 °C for 1 h (D). (B) hIGF-1 incubated with BME at a BME/IGF-1 ratio of 13/1 at 25 °C for 23 h. (1) IGF-1_{3S-S}, (1′) IGF-swap, (2) IGF-1_{1S-S}, and (3) IGF-1_{0S-S}.

peak and a decrease in the magnitude of the apoIGF-1 peak; the minor peak of the Cu_5IGF-1-BME form has appeared in the mass spectrum (Figure 8E). Mass analysis of Cu_4IGF-1 (assuming that four Cu^+ ions are bound) demonstrates that there are no disulfides in Cu_4IGF-1.

Characterization of hIGF-1 with HPLC. The gradient and solvent composition used by Miller et al.[34] were used with an Agilent Eclipse XDB C-18 column, and different hIGF-1 species have been resolved, providing results similar to those described previously.[34] A fully oxidized hIGF-1 sample exposed one major peak with retention at 31.7% B in reversed phase HPLC (Figure 9A, panel A). After incubation with 75 mM DTT for 1 h, hIGF-1 was fully reduced and hIGF-1_{0S-S} eluted at 36.6% B (Figure 9A, panel D). Disulfide rearrangement was initiated under our experimental conditions according to the procedure described by Miller et al.[34]

Equilibration of hIGF-1 under various redox conditions, similar to those used in ESI-MS experiments, was monitored by HPLC (Figure 9A, panels B and C). Three peaks were identified by ESI-MS to be major products of the reaction: peak 1 corresponding to hIGF-1_{3S-S}, peak 3 corresponding to hIGF-1_{0S-S}, and peak 2 corresponding to IGF-1 containing one disulfide bond (hIGF-1_{1S-S}). Retention times of these species were as follows: 31.7% B for IGF-1_{3S-S}, 36.1% B for IGF-1_{1S-S}, and 36.6% B for IGF-1_{0S-S}. IGF-1_{1S-S} is the major intermediate of the reaction in DTT/DTT_{ox} redox buffers under our experimental conditions. IGF-1_{2S-S} peaks were not detected in the course of the experiment, which suggests that both native disulfides of hIGF-1, 47−52 and 6−48, are reduced simultaneously and cooperatively. It has been shown earlier that prolonged incubation of IGF-1 under the conditions of extensive thiol exchange leads to the appearance of IGF with incorrectly folded disulfide bridges.[34] As seen in Figure 9B, after incubation of the BME/IGF-1 mixture for 23 h, the additional peak was eluted at 30.8% B, which corresponds to fully oxidized IGF-swap, nonnative product containing disulfide pairing (6−47, 18−61, 48−52). Such a peak was not detected in any of the chromatograms after incubation for 1 h (Figure 9A), suggesting that incorrect folding does not occur during our ESI-MS experiments.

DISCUSSION

The principal characteristic of the redox switching properties of the protein is the midpoint redox potential (E_m) of the redox processes involved. The E_m values can be determined from the equilibrium between oxidized and reduced forms of the protein at different environmental redox potential values maintained by GSH/GSSG or DTT/oxidized DTT redox buffers.[35] Importantly, high-resolution MS instruments allow the determination of the molecular mass of small proteins with an accuracy sufficient for direct monitoring of disulfide bond formation; thus, the redox equilibrium can be monitored without chemical modification of Cys residues.[28] In this work, we used a BME-based redox buffer instead of natural GSH as additional buffer to verify data obtained from the DTT redox system, because the nonionic BME is compatible with ESI-MS measurements and its redox potential is similar to that of GSH (−253 mV for BME and −262 mV for GSH).[32,36]

The ESI-MS studies reported here help us to understand the interplay between different redox states of hIGF-1. In general, our results exhibited a single sigmoid in the titration curve depending on the environmental conditions, suggesting that human IGF-1 exists mainly in two states corresponding to the fully oxidized and the reduced protein with six thiol groups whereas the latter can bind four Cu^+ ions. The high cooperativity of oxidative folding was confirmed by HPLC, showing that only a small amount (<20%) of the peptide with one disulfide bridge is forming at intermediate E_m values whereas the intermediate with two disulfide bonds is missing in all spectra. HPLC analysis also demonstrated the absence of

dx.doi.org/10.1021/bi300494s | Biochemistry 2012, 51, 5851−5859

misfolded hIGF-swap at redox equilibrium within the time course of the experiments.

We found that the E_m value of hIGF-1 oxidation is equal to −332 mV (at pH 7.5 and 40 °C). The extracellular redox environment in the living organisms is relatively oxidative: an E_h value of approximately −80 mV has been determined from the Cys/CySS ratio in the plasma of young healthy individuals.[16] The experimental midpoint redox potential value of IGF-1 is much lower than the extracellular E_h, which is in agreement with the presence of three disulfide bonds in the IGF-1 molecules in extracellular fluids.[6]

In several reports, a thermodynamic folding problem of IGF-1 in vitro[34,37] was observed under redox conditions with an E_h value for the GSH/GSSG system of around −335 mV. Our results show that under these conditions hIGF-1 is not fully oxidized and thus will not be able to acquire its native fold. Moreover, the redox state of the secretory pathway has recently been reported to be more oxidized, and the redox potential has been estimated to be −189 mV,[7] which ensures IGF-1 oxidation and complete disulfide formation in vivo.

Several attempts to study the structural aspects of IGF-1 and its interaction with the receptor and IGFBPs have been made. Three native disulfide bonds that were shown to be critical for binding of IGF-1 with the type I IGFR are between Cys6 and Cys48, Cys18 and Cys61, and Cys47 and Cys52.[6] The X-ray structure of the IGF-1 ternary complex with N- and C-terminal domain fragments of IGFBP-4 revealed the same disulfides in IGF-1.[38] Besides this, several other crystal structures (see for examples refs 39−41) and solution structures[42,43] of IGF-1 alone or in complex with IGFBPs have been published, and all these studies show that native disulfides are involved in the formation of the three-dimensional structure of hIGF-1, which is necessary for its recognition by other biomolecules.

The presence of thiol groups in reduced hIGF-1 suggests that it can potentially bind zinc and/or copper ions. Our results demonstrate clearly that fully reduced hIGF-1 does not bind Zn^{2+} ions (data not shown); however, the protein can bind four Cu^+ ions in a highly cooperative manner. The cooperative character of the binding is obvious from the absence of peaks corresponding to protein forms Cu_1IGF-1, Cu_2IGF-1, and Cu_3IGF-1 in the mass spectrum throughout the titration. These experiments show that fully reduced IGF-1 is a good model for proteins containing six Cys residues. It has been suggested that this type of protein preferentially binds four Cu^+ ions with tetracopper−hexathiolate cluster formation occurring during metal ion binding.[25−27] Our results confirm this suggestion and demonstrate that the binding of four copper ions requires the presence of six thiol groups in the protein and is sequence-independent.

Our results show that hIGF-1 can also form a complex with five Cu^+ ions. However, an additional thiol ligand is required for the binding of the fifth Cu^+ ion, because the peaks corresponding to five bound copper ions in the mass spectrum always contained DTT or BME (Figure 6C−E, peaks with asterisks). The results demonstrate that the Cu_5IGF-1 peak does not arise from the nonspecific binding of an excess of metal.

We used the titration of the metal form of the protein with DTT to estimate the affinity of hIGF-1 for copper ions. DDT at supramillimolar concentrations can extract metals from Cu_4IGF-1. On the basis of our results, the calculated K_d(Cu^+-hIGF-1) value is equal to $(3.00 \pm 0.86) \times 10^{-18}$ M. This value was calculated as previously described in ref 25 using the corrected K_d(Cu^+-DTT) value of 5×10^{-16} M.[44] To compare the Cu^+ binding affinity of fully reduced hIGF-1 with the copper chaperone for cytochrome *c* oxidase Cox17, the K_d(Cu^+-Cox17) from ref 25 was recalculated using the corrected K_d(Cu^+-DTT) and was found to be equal to 1.03×10^{-18} M. This comparison showed that the Cu^+ binding affinity of fully reduced hIGF-1 is 3-fold lower than that of Cox17, which has the lowest affinity among the cellular copper chaperones.[25]

Dietary copper has been shown to play a certain role in the regulation of IGF-1,[45,46] but there are no data about a direct interaction of hIGF-1 with Cu^+ ions. The majority of IGF-1, which circulates in extracellular fluids in complex with IGFBP-s or in an unbound fully oxidized form, is therefore unable to bind any metal ions. In the secretory pathway, the hIGF-1 molecules are most likely also oxidized considering the estimated redox potential of −189 mV for the ER.

The midpoint redox potential values are important determinants of the state of a protein within different compartments of the cell as well as in the extracellular matrix. It is important to note that intracellular and extracellular redox conditions are not absolutely stable and can fluctuate even under normal physiological conditions; usually, the potential becomes more oxidizing during different diseases and aging. In the case of IGF-1, the very low redox potential value keeps the protein in the native folded oxidized state; however, for a large number of proteins, the redox switches are physiologically very significant. In this paper, we demonstrate the applicability of the ESI-MS method for a complex investigation of the redox and metal binding properties using hIGF-1 as a relatively simple model protein. The observed results show that the method would be applicable also for more complex proteins.

AUTHOR INFORMATION

Corresponding Author

*Telephone: +372 620 4410. E-mail: peep.palumaa@ttu.ee.

Author Contributions

P.P. and J.S. designed the research. J.S. and J.M. performed the experiments. J.S., J.M., P.P., and V.T. analyzed the results, and the manuscript was written through contributions of all authors. All authors have given approval to the final version of the manuscript.

Funding

This work was supported by the Estonian Ministry of Education and Research (Grant SF0140055s08) and Estonian Science Foundation Grant 8811 (both to P.P.) and Estonian Science Foundation Grant 9318 to (V.T.).

Notes

The authors declare no competing financial interest.

ABBREVIATIONS

BME, 2β-mercaptoethanol; DTT, dithiothreitol; DTT_{ox}, oxidized dithiothreitol; ESI-MS, electrospray ionization mass spectrometry; GH, growth hormone; GSH, glutathione; hIGF-1, human insulin-like growth factor 1; IGF-1R, insulin-like growth factor 1 receptor; IGFBP, IGF binding proteins; ROS, reactive oxygen species; RNS, reactive nitrogen species; CyS/CySS, cysteine/cystine redox pair; ER, endoplasmic reticulum.

REFERENCES

(1) De Wolf, E., Gill, R., Geddes, S., Pitts, J., Wollmer, A., and Grotzinger, J. (1996) Solution structure of a mini IGF-1. *Protein Sci. 5*, 2193−2202.

(2) Lund, P. K. (1994) Insulin-like growth factor I: Molecular biology and relevance to tissue-specific expression and action. *Recent Prog. Horm. Res. 49*, 125−148.
(3) Jones, J. I., and Clemmons, D. R. (1995) Insulin-like growth factors and their binding proteins: Biological actions. *Endocr. Rev. 16*, 3−34.
(4) Baxter, R. C. (2000) Insulin-like growth factor (IGF)-binding proteins: Interactions with IGFs and intrinsic bioactivities. *Am. J. Physiol. 278*, E967−E976.
(5) Clemmons, D. R. (2007) Value of insulin-like growth factor system markers in the assessment of growth hormone status. *Endocrinol. Metab. Clin. North Am. 36*, 109−129.
(6) Narhi, L. O., Hua, Q. X., Arakawa, T., Fox, G. M., Tsai, L., Rosenfeld, R., Holst, P., Miller, J. A., and Weiss, M. A. (1993) Role of native disulfide bonds in the structure and activity of insulin-like growth factor 1: Genetic models of protein-folding intermediates. *Biochemistry 32*, 5214−5221.
(7) Hwang, C., Sinskey, A. J., and Lodish, H. F. (1992) Oxidized redox state of glutathione in the endoplasmic reticulum. *Science 257*, 1496−1502.
(8) Sen, C. K. (2000) Cellular thiols and redox-regulated signal transduction. *Curr. Top. Cell. Regul. 36*, 1−30.
(9) Hansen, J. M., Go, Y. M., and Jones, D. P. (2006) Nuclear and mitochondrial compartmentation of oxidative stress and redox signaling. *Annu. Rev. Pharmacol. Toxicol. 46*, 215−234.
(10) Jones, D. P. (2006) Redefining oxidative stress. *Antioxid. Redox Signaling 8*, 1865−1879.
(11) Moriarty-Craige, S. E., and Jones, D. P. (2004) Extracellular thiols and thiol/disulfide redox in metabolism. *Annu. Rev. Nutr. 24*, 481−509.
(12) Jones, D. P. (2006) Disruption of mitochondrial redox circuitry in oxidative stress. *Chem.-Biol. Interact. 163*, 38−53.
(13) Go, Y. M., and Jones, D. P. (2008) Redox compartmentalization in eukaryotic cells. *Biochim. Biophys. Acta 1780*, 1273−1290.
(14) Kemp, M., Go, Y. M., and Jones, D. P. (2008) Nonequilibrium thermodynamics of thiol/disulfide redox systems: A perspective on redox systems biology. *Free Radical Biol. Med. 44*, 921−937.
(15) Go, Y. M., and Jones, D. P. (2010) Redox clamp model for study of extracellular thiols and disulfides in redox signaling. *Methods Enzymol. 474*, 165−179.
(16) Blanco, R. A., Ziegler, T. R., Carlson, B. A., Cheng, P. Y., Park, Y., Cotsonis, G. A., Accardi, C. J., and Jones, D. P. (2007) Diurnal variation in glutathione and cysteine redox states in human plasma. *Am. J. Clin. Nutr. 86*, 1016−1023.
(17) Gilbert, H. F. (1990) Molecular and cellular aspects of thiol-disulfide exchange. *Adv. Enzymol. Relat. Areas Mol. Biol. 63*, 69−172.
(18) Huber-Wunderlich, M., and Glockshuber, R. (1998) A single dipeptide sequence modulates the redox properties of a whole enzyme family. *Folding Des. 3*, 161−171.
(19) Krause, G., and Holmgren, A. (1991) Substitution of the conserved tryptophan 31 in *Escherichia coli* thioredoxin by site-directed mutagenesis and structure-function analysis. *J. Biol. Chem. 266*, 4056−4066.
(20) Lin, T. Y., and Kim, P. S. (1989) Urea dependence of thiol-disulfide equilibria in thioredoxin: Confirmation of the linkage relationship and a sensitive assay for structure. *Biochemistry 28*, 5282−5287.
(21) Wunderlich, M., and Glockshuber, R. (1993) Redox properties of protein disulfide isomerase (DsbA) from *Escherichia coli*. *Protein Sci. 2*, 717−726.
(22) Ostergaard, H., Tachibana, C., and Winther, J. R. (2004) Monitoring disulfide bond formation in the eukaryotic cytosol. *J. Cell Biol. 166*, 337−345.
(23) Lopez-Mirabal, H. R., and Winther, J. R. (2008) Redox characteristics of the eukaryotic cytosol. *Biochim. Biophys. Acta 1783*, 629−640.
(24) Samiec, P. S., Drews-Botsch, C., Flagg, E. W., Kurtz, J. C., Sternberg, P., Jr., Reed, R. L., and Jones, D. P. (1998) Glutathione in human plasma: Decline in association with aging, age-related macular degeneration, and diabetes. *Free Radical Biol. Med. 24*, 699−704.
(25) Palumaa, P., Kangur, L., Voronova, A., and Sillard, R. (2004) Metal-binding mechanism of Cox17, a copper chaperone for cytochrome c oxidase. *Biochem. J. 382*, 307−314.
(26) Banci, L., Bertini, I., Ciofi-Baffoni, S., Janicka, A., Martinelli, M., Kozlowski, H., and Palumaa, P. (2008) A structural-dynamical characterization of human Cox17. *J. Biol. Chem. 283*, 7912−7920.
(27) Ahte, P., Palumaa, P., and Tamm, T. (2009) Stability and conformation of polycopper-thiolate clusters studied by density functional approach. *J. Phys. Chem. A 113*, 9157−9164.
(28) Zovo, K., and Palumaa, P. (2009) Modulation of redox switches of copper chaperone Cox17 by Zn(II) ions determined by new ESI MS-based approach. *Antioxid. Redox Signaling 11*, 985−995.
(29) Banci, L., Bertini, I., Ciofi-Baffoni, S., Kozyreva, T., Zovo, K., and Palumaa, P. (2010) Affinity gradients drive copper to cellular destinations. *Nature 465*, 645−648.
(30) Cleland, W. W. (1964) Dithiothreitol, a New Protective Reagent for SH Groups. *Biochemistry 3*, 480−482.
(31) Lees, W. J., and Whitesides, G. M. (1993) Equilibrium Constants for Thiol-Disulfide Interchange Reactions: A Coherent, Corrected Set. *J. Org. Chem. 58*, 642−647.
(32) Keire, D. A., Strauss, E., Guo, W., Noszal, B., and Rabenstein, D. L. (1992) Kinetics and equilibria of thiol-disulfide interchange reactions of selected biological thiols and related molecules with oxidized glutathione. *J. Org. Chem. 57*, 123−127.
(33) Schafer, F. Q., and Buettner, G. R. (2001) Redox environment of the cell as viewed through the redox state of the glutathione disulfide/glutathione couple. *Free Radical Biol. Med. 30*, 1191−1212.
(34) Miller, J. A., Narhi, L. O., Hua, Q. X., Rosenfeld, R., Arakawa, T., Rohde, M., Prestrelski, S., Lauren, S., Stoney, K. S., Tsai, L., et al. (1993) Oxidative refolding of insulin-like growth factor 1 yields two products of similar thermodynamic stability: A bifurcating protein-folding pathway. *Biochemistry 32*, 5203−5213.
(35) Dutton, P. L. (1978) Redox potentiometry: Determination of midpoint potentials of oxidation-reduction components of biological electron-transfer systems. *Methods Enzymol. 54*, 411−435.
(36) Millis, K. K., Weaver, K. H., and Rabenstein, D. L. (1993) Oxidation/reduction potential of glutathione. *J. Org. Chem. 58*, 4144−4146.
(37) Hober, S., Forsberg, G., Palm, G., Hartmanis, M., and Nilsson, B. (1992) Disulfide exchange folding of insulin-like growth factor I. *Biochemistry 31*, 1749−1756.
(38) Sitar, T., Popowicz, G. M., Siwanowicz, I., Huber, R., and Holak, T. A. (2006) Structural basis for the inhibition of insulin-like growth factors by insulin-like growth factor-binding proteins. *Proc. Natl. Acad. Sci. U.S.A. 103*, 13028−13033.
(39) Brzozowski, A. M., Dodson, E. J., Dodson, G. G., Murshudov, G. N., Verma, C., Turkenburg, J. P., de Bree, F. M., and Dauter, Z. (2002) Structural origins of the functional divergence of human insulin-like growth factor-I and insulin. *Biochemistry 41*, 9389−9397.
(40) Zeslawski, W., Beisel, H. G., Kamionka, M., Kalus, W., Engh, R. A., Huber, R., Lang, K., and Holak, T. A. (2001) The interaction of insulin-like growth factor-I with the N-terminal domain of IGFBP-5. *EMBO J. 20*, 3638−3644.
(41) Vajdos, F. F., Ultsch, M., Schaffer, M. L., Deshayes, K. D., Liu, J., Skelton, N. J., and de Vos, A. M. (2001) Crystal structure of human insulin-like growth factor-1: Detergent binding inhibits binding protein interactions. *Biochemistry 40*, 11022−11029.
(42) Cooke, R. M., Harvey, T. S., and Campbell, I. D. (1991) Solution structure of human insulin-like growth factor 1: A nuclear magnetic resonance and restrained molecular dynamics study. *Biochemistry 30*, 5484−5491.
(43) Sato, A., Nishimura, S., Ohkubo, T., Kyogoku, Y., Koyama, S., Kobayashi, M., Yasuda, T., and Kobayashi, Y. (1993) Three-dimensional structure of human insulin-like growth factor-I (IGF-I) determined by ^{1}H-NMR and distance geometry. *Int. J. Pept. Protein Res. 41*, 433−440.

(44) Xiao, Z., Brose, J., Schimo, S., Ackland, S. M., La Fontaine, S., and Wedd, A. G. (2011) Unification of the copper(I) binding affinities of the metallo-chaperones Atx1, Atox1, and related proteins: Detection probes and affinity standards. *J. Biol. Chem. 286*, 11047−11055.
(45) Roughead, Z. K., and Lukaski, H. C. (2003) Inadequate copper intake reduces serum insulin-like growth factor-I and bone strength in growing rats fed graded amounts of copper and zinc. *J. Nutr. 133*, 442−448.
(46) Jiang, Y., Reynolds, C., Xiao, C., Feng, W., Zhou, Z., Rodriguez, W., Tyagi, S. C., Eaton, J. W., Saari, J. T., and Kang, Y. J. (2007) Dietary copper supplementation reverses hypertrophic cardiomyopathy induced by chronic pressure overload in mice. *J. Exp. Med. 204*, 657−666.